INTERNATIONAL JOURNAL OF AGRICULTURE & BIOLOGY
ISSN Print: 1560–8530; ISSN Online: 1814–9596
19F–126/2020/23–2–381–390
DOI: 10.17957/IJAB/15.1299
http://www.fspublishers.org

Full Length Article

Effects of Advanced Glycation End Products on Rats Thymus and Thymic T Lymphocyte Subsets Differentiation

Wei Zhao[1], Xingzhou Li[1], Jialin Li[1], Changsan Wang[1], Shimin Zheng[2*] and Tianming Jin[3*]
[1]*Jiamusi University, Jiamusi, Heilongjiang Province 154007, P. R. China*
[2]*College of Veterinary Medicine, Northeast Agricultural University, Harbin, Heilongjiang Province 150030, P. R. China*
[3]*College of Animal Science and Veterinary Medicine, Tianjin Agricultural University, Tianjin 30084, China*
[*]For correspondence: zhengshiminbl@sohu.com; JTMSCI@163.com
Received 01 July 2019; Accepted 18 September 2019; Published 16 January 2020

Abstract

The aims of this study were to investigate the role of advanced glycation end products (AGEs) and their specific receptor {receptor for advanced glycosylation end products (RAGE)} in the rat thymus and in thymocyte differentiation. *Invitro*, AGEs (AGE-modified rat serum albumin) were prepared by incubating rat serum albumin with D-glucose. Rat tail veins were injected with AGEs and 45 days later; the rats were sacrificed. Thymic AGE levels induced by AGEs increased significantly comparison with the young control ($P < 0.01$). The morphology, T lymphocyte number, and T lymphocyte proliferation ability of the thymus in rats treated with AGEs showed regressive changes similar to those in the aging control group ($P < 0.05$), and the differentiation of T lymphocyte subsets was consistent with aging in the rats ($P < 0.05$). In the thymus, the levels of *Rage* mRNA were enhanced in AGE-treated rats, while *Notch1* mRNA levels decreased significantly. The mRNA changes detected by quantitative real time RT-PCR were confirmed using western blotting. In conclusion, our data suggested that AGEs caused regressive changes in the thymus, and the RAGE signaling pathway plays an important role in the thymic differentiation of T lymphocyte subsets. © 2020 Friends Science Publishers

Keywords: Advanced glycation end products: Rats; Thymus; Thymic T lymphocyte subsets differentiation; Immunosenescence

Introduction

The thymus, a major lymphoid organ, undertakes the homeostatic maintenance of the peripheral immune system. In the thymus gland, naive T cells, which mediate humoral and cellular immunity, develop and are processed for export to the periphery, where they establish a functional immune system (Lynch *et al.* 2009). The ageing-related reduction in the efficiency of the immune system has direct etiological links with an increase in diseases such as opportunistic infections, autoimmunity, and the incidence of cancer. Shrinkage of the thymus gland is believed to be a major factor in age-related loss of immune function (Gruver *et al.* 2007).

The non-enzymatic glycation of the amino groups on proteins, lipids, and nucleic acids with reducing sugars, e.g., glucose and galactose, produce advanced glycation end products (AGEs). It has been suggested that AGEs are responsible for pathological features associated with diabetes, uremic complications, atherosclerosis, amyloidosis, and aging (Neeper *et al.* 1992). Advanced glycation end products form protein cross-links in the extracellular matrix that alter its structure and function and interact with specific receptors on the cell surface. Receptor for advanced glycosylation end products (RAGE) is the best-characterized AGE receptor (Yan *et al.* 1994). Increased production of cytokines, including transforming growth factor beta (TGFβ), mitogen-activated protein kinases (MAPKs) (Li *et al.* 2004; Leclerc *et al.* 2007), Jun-N-terminal kinase (JNK), p38, and extracellular signal-regulated kinases (ERK) (Stern *et al.* 2002), result from the interactions between AGEs and their binding proteins.

Advanced glycation end products accelerate and exacerbate the aging process, contributing to the initial phases of age-related diseases, such as cataracts, atherosclerosis, renal failure, neurodegenerative disease, age-related macular degeneration, and arthritis (Tian *et al.* 2005). The aging heart is susceptible to the glycation processes; the consequences of which may result in ventricular dysfunction, altered regulation of vascular tone, and increased ventricular and vascular stiffness (Lakatta and Levy 2003). Advanced glycation end products accumulated in glaucomatous tissues support the view that an accelerated aging process accompanies neurodegeneration in glaucomatous eyes (Tezel *et al.* 2007). It has been reported that immune system aging induced by D-galactose results

from the effect of non-enzymatic glycation *invivo*, and produces retrogressive morphological changes to the ultrastructure of the thymus and spleen lymphocytes, and decreases lymphocyte proliferation and IL-2 activity in the spleen (Deng *et al*. 2006). The direct thymic effect of AGEs and the differentiation of subsets of T cells have not yet been reported.

Thus, the present study focused on the effects on the thymus of injecting AGEs prepared *invitro* into rats *via* their tail veins, in comparison with rats treated with ALT-711 (also known as Alagebrium, a 4,5-dimethylthiazolium derivative of N-phenyl-thiazolium bromide, which is stable and can cleave established AGE cross-links (Vasan *et al*. 1996). The present study aimed to address whether AGEs could cause changes in thymic structures, especially alterations to the differentiation of T lymphocyte subsets and, furthermore, to explore the mechanism of any changes observed.

Materials and Methods

Reagents

4,5-dimethyl-3-(2-oxo-2-phenyl ethyl)-thiazol-3-ium chloride (ALT-711) was purchased from Paul Wakfer (Canada), and Sigma Chemical Co. (St. Louis, M.O., U.S.A.) provided the D-glucose. The analytical agents glutaral, hydrogen osmate, Epon812, dimethyl formamide, and dimethyl sulfoxide were purchased from Shanghai Reagent Factory (Shanghai, China). Antibodies, including fluorescein isothiocyanate (FITC)-mouse anti-rat CD3, phycoerythrin (PE)-mouse anti-rat CD4, and peridinin chlorophyll protein complex (PerCP)-mouse anti-rat CD8a were obtained from BD Pharmingen (San Jose, C.A., U.S.A.). Rabbit anti-RAGE, rabbit anti-Notch1, rabbit anti-β-Actin, and horseradish peroxidase (HRP)-conjugated Goat Anti-Rabbit IgG(H+L) were obtained from BD Pharmingen. Trizol, the SYBR ®PrimeScript™ RT-PCR Kit II, and the PrimeScript™ RT-PCR reagent Kit were obtained from Takara (Shiga, Japan).

In vitro preparation of ligands

Advanced glycation end product-modified rat serum albumin (RSA) was prepared by incubating RSA (5 mg/mL) at 37°C for 12 weeks with D-glucose (0.5 mol/L) in 0.2 mol/L phosphate buffer (pH 7.4) with 100 U/mL each of penicillin and streptomycin (added after filter sterilization). Controls comprised RSA samples incubated in an identical manner in the absence of glucose. To remove unreacted D-glucose, the samples were dialyzed extensively against phosphate buffered saline (PBS) and then lyophilized. The endotoxin concentration, as determined using the tachypleus amebocyte lysate method (according to the second edition of the Chinese Pharmacopoeia 2005 edition). Advanced glycation was assessed *via* its characteristic fluorescence (excitation at 370 nm, emission at 440 nm) (Soulis-Liparota *et al*. 1991).

Animals and treatments

Animals were housed in facilities conforming to international guidelines, and the study was approved by the Ethics Committee of the Jiamusi University (permit number: JMSU-20170018)

Female Sprague-Dawley pathogen-free rats (2 months old; Harbin Veterinary Research Institute of Chinese Academy of Agricultural Science) were divided randomly into four groups (n = 8 per group). Rats were given standard rat feed and chemical composition of feed was determined as described in literature (Arslan and Culpan 2017; Hassan *et al.* 2017; Vasileva and Naydenova 2017; Zulfiqar *et al.* 2017). The rats were allowed to adapt for one week before being treated with one of the following preparations daily for 45 days (*via* tail vein injection): The young control group were treated 1 mL of PBS as a vehicle control; the RSA control group comprised 2-month-old rats treated with 100 mg/kg RSA; the AGE+ALT-711 group comprised 2-month-old rats treated with 100 mg/kg AGE-RSA plus ALT-711 at 10 mg/kg per os; and the AGE group, as the model group, comprised rats treated with 100 mg/kg AGE-RSA. The fifth group, comprising aged rats (16 months old), were given 1 mL of PBS daily *via* tail vein injection as an aging control. At the end of the experiment, the rats were humanely sacrificed. Their tissues and organs were excised promptly and used immediately in experiments or stored at −70°C for later use.

Determination of AGE levels in thymus

According to the method of Monnier *et al.* (1986), tissue (25 mg) was homogenized for 60 sec with 5 mL of PBS (pH 7.4) followed by centrifugation at 4,700 × *g* for 30 min at 4°C. The pellets were washed three times with demineralized water, and rehydrated in 2.5 mL of 2:1 chloroform-methanol for 24 h at 4°C. The samples were dissolved in 10 mL of methanol and 250 μL of water, followed centrifugation at 4,700 × *g* at 4°C for 30 min. The tissue pellets were washed two times with 1 mL of 0.1 mol/L $CaCl_2$ (including 150 U of type VII collagen) with 1 μL of chloroform and 1 μL of toluene, while the blank control comprised 0.1 mol/L $CaCl_2$ (including 150U type VII collagen); all samples were incubated for 24 h at 37°C. All samples were then centrifuged, and supernatants were removed. Pellets were rehydrated in 1 mL $CaCl_2$ (0.1 mol/L, including 150 U of type VII collagen) with 1 μL of chloroform and 1 μL of toluene, while the blank comprised 0.1 mol/L $CaCl_2$ (including 150 U type VII collagen); all samples were incubated for 24 h at 37°C. All samples were then centrifuged at 7,100 × g for 5 min at 4°C. The supernatants were assessed for advanced glycation-related fluorescence (excitation at 370 nm; emission at 440 nm)

(Soulis-Liparota *et al.* 1991). The extent of advanced glycation was calculated as fluorescence dose in 1 mg of protein (arbitrary unit of fluorescence (AUF)/mg. protein).

Light and transition electron microscopy of the ultrastructure of the thymus

After the animals were sacrificed, the thymus was removed under sterile condition, fixed immediately in 4% glutaral and 1% hydrogen osmate for transmission electron microscopy and in 10% formaldehyde for light microscopy, respectively. The samples for light microscopy (hematoxylin and eosin (H&E) stained) were treated with Xylene I, II, and III (5 min) for deparaffinization; rehydrated for 5 min in 100%, 100%, 95%, 95%, 80% and 70% alcohol, successively; rinsed in distilled water for 5 min; stained with hematoxylin for 5 min; rinsed; deparaffinized in for 5 min in Xylene I, II, and III; incubated for 5 min in 100%, 100%, 95%, 95%, 80% and 70% alcohol, successively, for rehydration; rinsed in distilled water for 5 min; stained with hematoxylin for 5 min; rinsed for 20 min in running tap water; decolorized for 5 min in acid alcohol; rinsed for 5 min in tap water; immersed in Eosin (15 seconds); dehydrated for 5 min in 80%, 95%, and 95% alcohol; cleared for 5 min in Xylene I and II; placed in a fume hood and mounted using Cytoseal; and then observed and photographed using a BI-2000 medical imaging analytical system.

The samples for transmission electron microscopy were dehydrated for 10 min in 50%, 70%, 80%, 90%, 95% alcohol, and 95% alcohol:95% acetone (V/V=1:1) successively; dehydrated for 40 min with 100% acetone; infiltrated for one hour with epoxypropane and epoxy resin (V/V=1:1); embedded with Epon812; and aggregated for 12 h at 35, 45, and 55°C, successively. The cells were then cut into 70 nm slices using an LKB-III microtome (Japan), stained with uranyl acetate and lead citromalic acid, observed, and photographed under a JEM-1200EX transmission electron microscope (Japan).

Thymocyte T lymphocyte number detection

After the animals were sacrificed, their thymuses were quickly excised and paraffin sections were made. As described in Mueller *et al.* (1975), alfa-naphthyl acetate esterase (ANAE) was used to stain the sections, and the number of lymphocytes in different regions of the tissue per unit area (100 mm^2) was examined using oil immersion microscopy.

Thymic T lymphocyte proliferation function test

A sterile single cell suspension was prepared from thymocytes rapidly. The thymocytes were separated by density gradient centrifugation (450 × *g*, 20 min), and then washed with Roswell Park Memorial Institute (RPMI) 1640 medium (360 × g, 15 min) three times. Cell viability, which was detected using the trypan blue exclusion method, was greater than 95%. The cells were counted, and the cell concentration were adjusted to 1×10^7/mL. Then, to each well of a 96-well microplate, 50 μL of RPMI1640 medium with 20 μg/mL ConA was added; only RPMI1640 medium was added to the control wells. Then, to each well, lymphocyte suspension (50 μL) was added, resulting in a total culture volume of 100 μL in which the final concentration of the cells was 0.5×10^7/mL and the final concentration of Con A was 10 μg/mL; three sets of replicate wells were used. The cells in the plates were cultured for 45 hours at 40°C, 5% CO_2, and saturated humidity. Thereafter, 10 μL of 3-(4,5-dimethylthiazol-2-yl)-2,5-diphenyltetrazolium bromide (MTT; 5 mg/mL) was added to each well and culture was continued for 3 h. Subsequently, to each well, DMSO (100 μL) was added and the plates were incubated for 15 min at 37°C. The cells were then subjected to an enzyme-linked immunosorbent assay, with the blank control well treated as zero. The absorbance value (A590 nm) was expressed as the average of three replicate wells.

Isolation of thymus cells

Thymus samples were pressed through a 200-mesh stainless steel screen and then filtered through a 300-mesh steel screen to remove the unfractured tissues. A single cell suspension of thymic lymphocyte was generated using Ficoll 400. Phosphate-buffered saline (10 mL) supplemented with 2% bovine serum albumin (BSA) was used to wash the cells, which were then centrifuged for 10 min at 450 × g and 4°C. Phosphate-buffered saline with 2% BSA (1 mL) was used to re-suspend the cell pellets, which were then counted and adjusted to 1×10^7 cells/tube.

Flow cytometry analysis

Isolated thymus cells were added to cytometry tubes (100 μL, 1×10^6 cells/tube) and incubated with monoclonal antibodies for 30 min at room temperature. The following monoclonal antibodies were used for T cell subsets analysis: FITC-conjugated mouse anti-rat CD3, PE-conjugated mouse anti-rat CD4, and PerCP-conjugated mouse anti-rat CD8a. After incubation, the cells were washed by centrifugation at 450 × *g* for 10 min at room temperature. Prior to detecting lymphocyte subsets, the cell pellets were suspended in 400 μL of PBS containing 2% BSA. A FACScan (Becton Dickinson, Palo Alto, CA, USA) was used to acquire the data, after compensation using single-labeled cells and control antibodies. The FCS Express program, using the fluorescence intensity data, was used to calculate percentage of positively stained cells.

Quantitative real-time reverse transcription PCR

The Trizol reagent (Takara) was used to extract total RNA from thymus tissue, which then used as a template to produce cDNA using the PrimeScript™ RT-PCR reagent Kit (Takara). QPCR was executed using the SYBR ®PrimeScript™ RT-PCR Kit II (Takara). PCR primers for *Rage* and *Notch1* were designed using Primer Express software (ABI, Foster City, C.A., U.S.A.) and sequence data contained within the National Center for Biotechnology Information database. The rat *Rage* fragment (101 bp) PCR primers were 5'-CTCCTGTCAACATCAGGGTCAC-3' (forward) and 5'-GATCCCTAAGGCCAGGGCTA-3' (reverse), for the rat *Notch1* fragment (119 bp) were 5'-GTGCCTGTCTGAGGTCAACGA-3' (forward), and 5'-TGTCACAGTTTGTCCCACTCCA-3' (reverse), and for the rat *Actb* fragment (beta actin; 150 bp) were 5'-GGAGATTACTGCCCTGGCTCCTA-3'(forward) and 5'-GACTCATCGTACTCCTGCTTGCTG-3'(reverse). Briefly, the reaction mixture was prepared in PCR tubes following the manufacturer's instructions and placed into the ABI 7300 System (Applied Biosystems, Foster City, C.A., U.S.A.), and all PCR reactions were performed in triplicate. The RT-PCR procedure comprised reverse transcription (37°C for 15 min, 85°C for 5 sec.), PCR activation (50°C for 2 min), followed by 40 cycles of 95°C for 30 sec, 95°C for 5 sec, and 60°C for 30 sec for actin (61°C for *Rage* and *Notch1* PCR annealing temperature). PCR specificity was confirmed by dissociation curve analysis and gel electrophoresis. The qRT-PCR data were used to calculate expression of the target mRNA relative to that of *Actb*.

SDS-PAGE and western blotting

Total proteins were extracted from thymus tissues and quantitated using the bicinchoninic acid method. Equal amounts of protein samples (45 mg) from each group were loaded onto each lane of gels and then electrophoresed through Tris-glycine polyacrylamide (8–12%) gels. The separated proteins were electrophoretically transferred onto polyvinylidene difluoride membranes (Millipore Corp., Marlborough, MA, USA). Non-specific binding was blocked by incubating the membrane for 2 h at room temperature in 5% skim milk in tris-buffered saline with Tween-20 (TBST). Incubation of the membranes with primary antibodies took place overnight at 4°C, including rabbit anti-β-actin (1:600 dilution with TBST), rabbit anti-RAGE (1:1,000 dilution with TBST), and rabbit anti-Notch1 (1:1,000 dilution with TBST). After washing with TBST, the membranes were incubated for 1 h at room temperature with the HRP-conjugated goat anti-rabbit IgG (H+L) diluted 1:2000 in TBST. Tris-buffered saline with Tween-20was used to wash the membranes and the enhanced chemiluminescence (ECL) was used to visualize the immunoreactive protein bands before being exposed to Kodak X light film. The results in each lane were normalized band intensity of β-actin. The bands on the western blot were scanned using a Bio-Rad ChemiDoc XRS imager (Bio-Rad Hercules, C.A., U.S.A.), followed by quantification using BandScan 5.0 software (Shanghai Furi Company, Shanghai, China).

Data analysis

Data are presented as the mean ± standard error of the mean (SEM). Comparisons between groups were tested using one-way analysis of variance (ANOVA) analysis. SNK-q test was used for comparison between any two groups. *P* values < 0.05 were considered statistically significant.

Results

***In vitro* preparation of ligands**

The endotoxin concentration AGE-modified RSA was less than 0.125 EU/mL. Advanced glycation was assessed *via* its characteristic fluorescence (excitation at 370 nm, emission at 440 nm), and an approximately nine-fold increase in fluorescence resulting from advanced glycation was observed compared with the controls.

Body weight and thymus age levels in-vitro preparation of ligands

No significant changes to the body weight were observed in the young, RSA, AGEs and AGE+ALT-711 rats in pre-treatment and post-treatment ($P > 0.05$) (Table 1). The thymus AGE levels showed no changes in the young control and RSA control groups, which were treated with PBS and RSA, respectively ($P > 0.05$). In the rats treated with AGE-RSA (AGE group) and the aging control group, AGE levels were significantly higher than those in the young control group ($P < 0.01$). ALT-711 treatment prevented the increase in AGE levels compared with that in the AGE group ($P < 0.01$) (Table 1).

Morphological changes to the thymus

No significant changes to the thymic cortex thickness were observed in the young, RSA, and AGE+ALT-711 rats (Fig. 1, A-1, B-1, C-1). The thymic cortex of aging rats was significantly thinner and the rats treated with AGEs had aging-mimetic changes (Fig. 1, D-1, E-1) (Table 2). The ultrastructure of the thymus in each group showed that the lymphocytes in the thymus of young rats were round with large nuclei, and the mass of heterochromatin was found in the cell nuclei. The cytoplasm had many structurally normal mitochondria, with clear nucleoli (Fig. 1, A-2). The structures of the thymocytes in the RSA control and AGE+ALT-711 group were almost normal, and their ultrastructure was like that of the young control rats (Fig. 1, B-2, C-2). The lymphocyte nuclei in the thymus of old rats were irregular, with visible pyknosis and chromatin

Table 1: Levels of Thymus AGEs and the changes in body weight

Group	Number	Body Weight (g)		AGE
		Pre-treatment	Post-treatment	(AUF/mg.protein)
Young Control	8	212.12±14.48[a]	270.25±18.53[a]	6.68±1.38[a]
RSA Control	8	211.12±16.57[a]	273.25±16.18[a]	7.01±1.32[a]
AGE+ALT-711	8	212.00±15.12[a]	271.37±18.03[a]	13.14±0.89[c]
AGE Group	8	212.25±15.25[a]	273.75±15.57[a]	22.18±2.18[e]
Aging Control	8	616.12±18.85[c]	623.00±16.75	21.29±2.83[e]

Note: The values with different letter differ significantly (with consecutive letter, $P < 0.05$) or very significantly (with interval letter, $P<0.01$) and differ quietly (with same letter or unlabeled, $P > 0.05$). AGE, advance glycation end products; RSA, rat serum albumin; AUF, arbitrary unit of fluorescence; ALT-711, 4,5-dimethyl-3-(2-oxo-2-phenyl ethyl)-thiazol-3-ium chloride

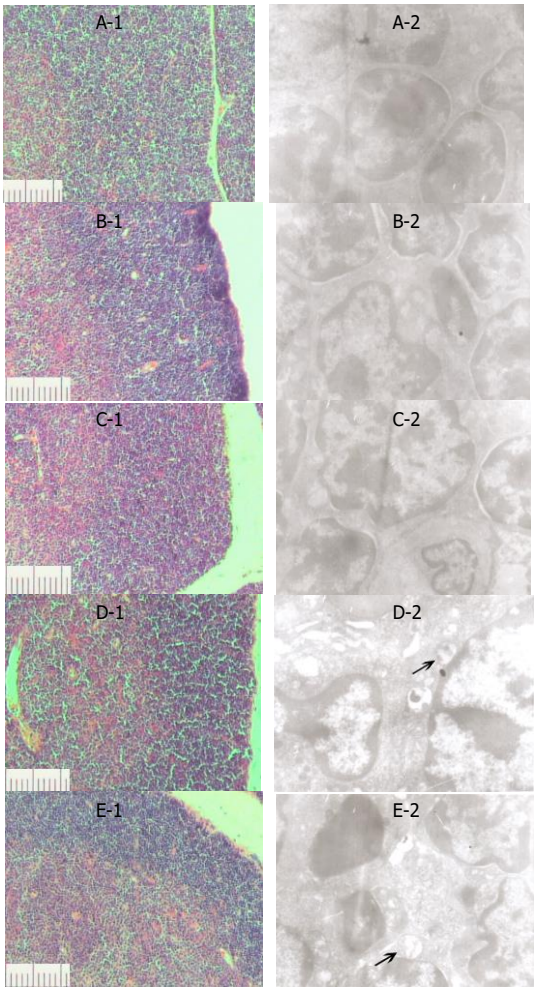

Fig. 1: Morphology Changes of Thymus in each group. **A-1**, H&E stain of young control rats (10×); **A-2**, Ultrastructure of young control rats (6000×); **B-1**, H&E stain of RSA control rats; **B-2**, Ultrastructure of RSA control rats (6000×); **C-1**, H&E stain of AGEs+ALT-711 control rats (10×); **C-2**, Ultrastructure of AGEs+ALT-711 control rats (8000×); **D-1**, H&E stain of AGEs rats (10×); **D-2**, Ultrastructure of AGEs rats (8000×); **E-1**, H&E stain of aging control rats (10×); **E-2**, Ultrastructure of aging control rats (8000×). Minimum scale is 0.01 millimetre

margination. The cristae of the mitochondria were broken and swollen with vacuoles, and there were increased amounts of rough endoplasmic reticulum (Fig. 1, E-2). The thymocytes in rats treated with AGEs had an aging-mimetic ultrastructure. The irregular lymphocyte nuclei appeared as condensed intranuclear chromatin and chromatin margination. The cristae of mitochondria were broken and showed vacuolization (Fig. 1, D-2).

Changes in the number of thymus T lymphocytes

Compared with young control, there was no significant difference in the number of thymus T lymphocytes in RSA rats ($P > 0.05$). There were significantly fewer thymus T lymphocytes in the AGEs+ALT-711-treated rats ($P < 0.05$), AGE-treated rats ($P < 0.01$) and the aged rats ($P < 0.01$) compared with those in the young control rats. The thymus T lymphocyte count in the AGEs+ALT-711 rats increased significantly compared with that in the AGEs rats, ($P < 0.01$) (Table 3).

Changes of proliferation function of thymus T lymphocytes

The proliferation indices of the thymus T lymphocytes in the different groups stimulated by ConA were detected. The results are shown in Table 4. Compared with young rats, there was no significant difference in thymus T cell stimulation index of RSA rats ($P > 0.05$), while the stimulation index of thymus T cells of the AGEs+ALT-711-treated rats decreased significantly ($P < 0.05$). The stimulation index of thymus T cells also decreased significantly in the old rats ($P < 0.01$). The AGE-treated rats had similar changes to the aged rats, and their thymus lymphocyte stimulation index was lower. The young rats had significantly higher thymus T cell stimulation indexes ($P < 0.01$). Compared with the AGEs rats, the stimulation index of thymus T cells of the AGEs+ALT-711-treated rats increased significantly ($P < 0.01$).

Changes to lymphocyte subsets

We observed typical differences in the proportions of the principal thymocyte populations between the young and old thymus samples. A significant increase in the percentage of double-negative (DN) and single-positive (SP) $CD4^+$ thymocytes, and a significant decrease in double-positive (DP) and SP $CD8^+$ thymocytes were observed in aged rats in comparison with the young control group ($P < 0.01$) (Fig. 2). There was no significant variation of T lymphocyte subsets in the RSA control and AGE+ALT-711 group compared with those in the young group ($P > 0.05$). The proportion of DN and SP $CD4^+$ thymocytes of the AGE group was higher than that in the young control group, and the percentage of DP and SP $CD8^+$ cells in the AGE group was lower than that in the young control group ($P < 0.01$ or $P < 0.05$). We observed that in comparison with the young control rats, the variation in the number T lymphocytes in the AGE group was similar to that in the aging control

Table 2: The Thymic cortex thickness of rats in each group

Group	Number	Thymic cortex thickness (μm)
Young Control	8	203 ± 11.89a
RSA Control	8	206 ± 10.68a
AGEs+ALT-711	8	198 ± 15.16 a
AGE Group	8	115 ± 8.49 c
Aging Control	8	108 ± 7.35 c

Note: The values with different letter differ significantly (with consecutive letter, $P < 0.05$) or very significantly (with interval letter, $P < 0.01$) and differ quietly (with same letter or unlabelled, $P > 0.05$). AGE, advance glycation end products; RSA, rat serum albumin; AUF, arbitrary unit of fluorescence; ALT-711, 4,5-dimethyl-3-(2-oxo-2-phenyl ethyl)-thiazol-3-ium chloride

Table 3: Changes of the number of T cells of rats in each group

Group	Number	Thymus (× 103/mm2)
Young Control	8	6.67 ± 0.48^{a}
RSA Control	8	6.21 ± 0.44^{ab}
AGEs+ALT-711	8	6.06 ± 0.47^{b}
AGE Group	8	4.37 ± 0.49^{d}
Aging Control	8	2.70 ± 0.37^{f}

Note: The values with different letter differ significantly (with consecutive letter, $P < 0.05$) or very significantly (with interval letter, $P < 0.01$) and differ quietly (with same letter or unlabelled, $P > 0.05$). AGE, advance glycation end products; RSA, rat serum albumin; ALT-711, 4,5-dimethyl-3-(2-oxo-2-phenyl ethyl)-thiazol-3-ium chloride

Table 4: Changes of T-lymphocyte proliferative function in the thymus of rats in each group

Group	Number	Thymus (590 nm OD)
Young Control	8	2.66 ± 0.23^{a}
RSA Control	8	2.56 ± 0.22^{a}
AGEs+ALT-711	8	2.35 ± 0.24^{b}
AGE Group	8	1.21 ± 0.12^{d}
Aging Control	8	1.01 0.07 ^{d}

Note: The values with different letter differ significantly (with consecutive letter, $P < 0.05$) or very significantly (with interval letter, $P < 0.01$) and differ quietly (with same letter or unlabelled, $P > 0.05$. AGE, advance glycation end products; RSA, rat serum albumin; ALT-711, 4,5-dimethyl-3-(2-oxo-2-phenyl ethyl)-thiazol-3-ium chloride

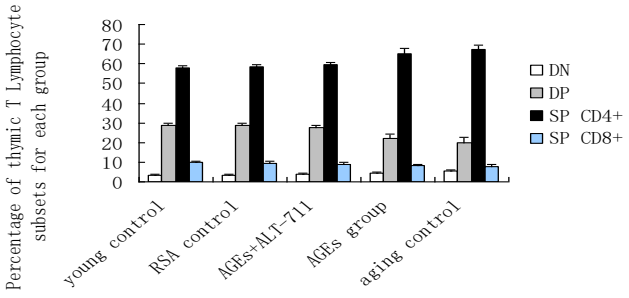

Fig. 2: The distribution of thymocyte populations in the different groups. DN, double-negative thymocytes, $CD4^{-}CD8^{-}$; DP, double positive thymocytes, $CD4^{+}CD8^{+}$; SP $CD4^{+}$, single-positive thymocytes, $CD4^{+}CD8^{-}$; SP $CD8^{+}$, single-positive thymocytes, $CD8^{+}CD4^{-}$. Statistically significant differences in the percentage of positive cells between old and young rats, and the varying tendency of T lymphocyte in AGEs group are consistent with the aging control in comparison with the young control

group (Fig. 3). In particular, the percentage of SP $CD4^{+}$ and DP cells in the AGE+ALT-711 rats was significantly different to that in the AGE rats ($P < 0.01$), which indicated that ALT-711 played an important role in the variation of T lymphocyte subsets in this study. The CD4:CD8 ratio in the AGE and aging groups was higher than that in the young and RSA groups, and ALT-711 could reverse this tendency significantly (Table 5).

Detection of rage and Notch1 expression in the thymus

To better understand the role of AGEs in the thymus and in and T lymphocyte differentiation we examined the expression of the *Rage* and *Notch1* in the thymus. The levels of *Rage* and *Notch1* mRNA in individual groups were quantitated using qRT-PCR. The PCR products were analyzed using dissociation curves and gel electrophoresis (Fig. 4). The results showed that the levels of *Rage* and *Notch1* mRNA were similar in the young control, RSA control, and AGE+ALT-711 groups ($P > 0.05$). Significantly higher *Rage* mRNA levels were observed in the AGE group and aging group compared with those in the young control group ($P < 0.01$). The level of *Rage* mRNA in the group treated with AGE+ALT-711 was much lower than that in the AGE group ($P < 0.01$) (Table 3), and the change in the mRNA level was consistent with the variation in protein levels in each group (Fig. 6). However, the levels of *Notch1* mRNA in each group showed the opposite tendency (Fig. 5). *Notch1* mRNA expression in the AGE rats and old rats was lower than that in the young rats. ALT-711 inhibited the decreased in *Notch1* mRNA expression in the AGE+ALT-711 rats in comparison with that in the AGE rats ($P < 0.05$) (Table 6). The qRT-PCR results confirmed those obtained using western blotting (Fig. 6).

Discussion

The thymus is a major immune organ that secretes thymosin to regulate T cell maturity and the function of immune system. It is generally accepted that the thymus undergoes marked retrogressive changes with aging, including weight loss and structural changes, such as involution, reduced numbers of lymphocytes and epithelial-reticular cells, disrupted cell membrane integrity, swollen mitochondria, disrupted crystae, and increased numbers of lysosomes. In the aging body, the absolute number of lymphocytes and their capacity to respond to antigenic stimuli are reduced. Despite repeated antigen stimulation, the production of immune cells was still reduced, which seriously affected the body's immune function (Surh and Sprent 2008). Age-related structural and functional changes to the thymus lead to decreases in naive T cell populations, and increased susceptibility to infectious diseases, cancer, and age-associated autoimmune diseases. These overall changes in the thymus form part of immunosenescence (Caruso *et al.* 2009).

Our study demonstrated that AGE levels in the thymus of rats treated with AGE-RSA increased significantly, and

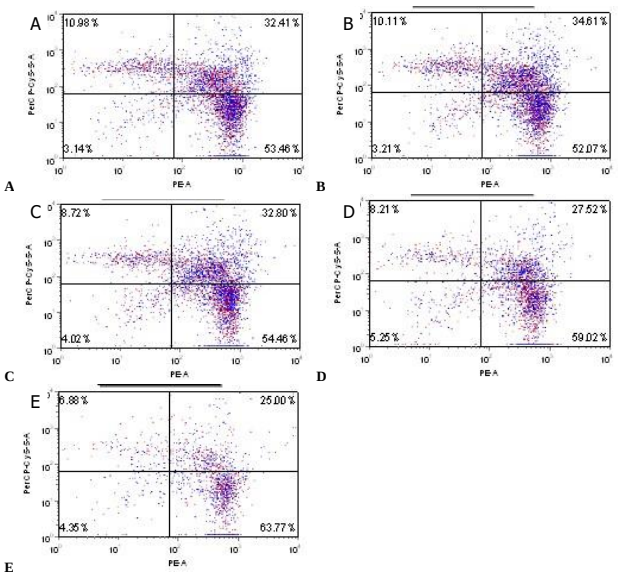

Fig. 3: The result of flow cytometry analysis for thymic T lymphocytes. A, young control rats; B, RSA control rats; C, AGEs+ALT-711 group rats; D, AGEs group rats; E, Aging control rats. Upper left quadrant, the percentage of SP CD8 cells; upper right quadrant, the percentage of DP cells; lower right quadrant, the percentage of SP CD4 cells; lower left quadrant, the percentage of DN cells. The sum total of the four quadrants is 100%. Each T lymphocyte subset is defined as follows: $CD4^+$ =PE positive T cells; $CD8^+$ = PerCP-positive T cells; $CD4^+CD8^+$ = PE and PerCP-positive T cells; DN = PE and PerCP negative

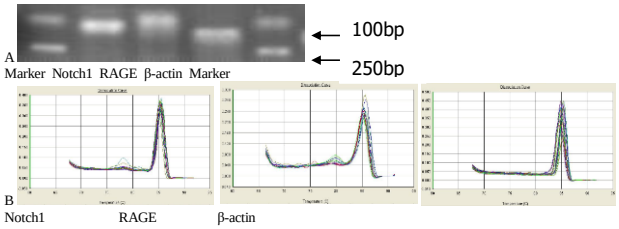

Fig. 4: The results of dissociation curve analysis and gel electrophoresis. **A**, gel electrophoresis of each gene; **B**, dissociation curve for each gene

the thickness of thymic cortex and the ultrastructure of thymus gland showed retrogressive morphological changes compared with the rats in the young and RSA groups. The AGE-treated rats showed the phenomenon of early apoptosis and chromatin margination. In addition, AGEs affected the T lymphocyte count in the rat thymus and reduced the proliferation of immune organ T lymphocytes. Such changes are correspond to the aging process. To further clarify the effect of AGEs on the thymus, a group of Sprague-Dawley rats treated with AGEs received ALT-711, a cross-link breaker. ALT-711 has been shown to cleave preformed AGEs (Vasan *et al*. 1996) and can reduce AGE accumulation in the context of diabetes (Cooper *et al*., 2000). Diabetic rats treated with ALT-711 showed

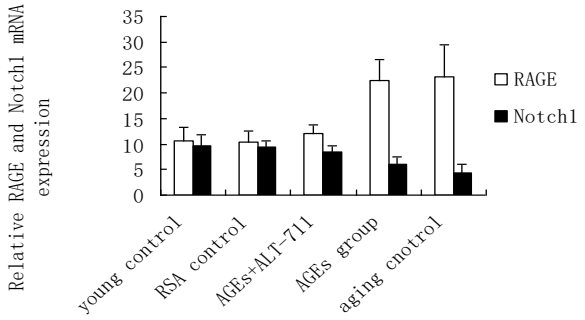

Fig. 5: Changes in *Rage* and *Notch1* mRNA relative expression in each group

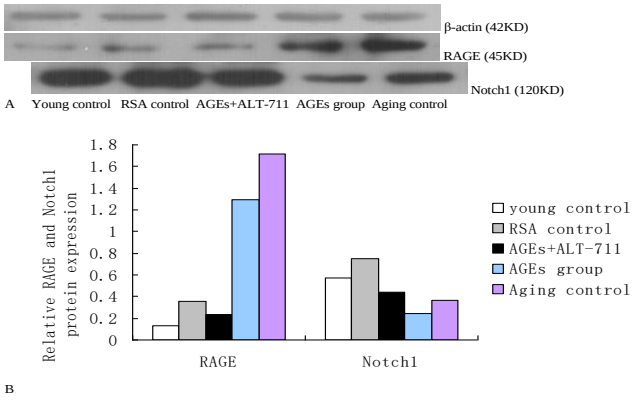

Fig. 6: Western blotting analysis of RAGE and Notch1 proteins in the various groups. A, The RAGE protein levels in the AGEs group and the aging control group were significantly higher than those in the other groups; the Notch1 protein level showed the reverse tendency. B, Relative RAGE and Notch1 protein levels. Relative levels of the proteins were normalized to the β-actin levels in each group

improved vascular compliance (Wolffenbuttel *et al*. 1998). Our results suggested that the aging effect of the thymus was induced by AGEs, providing a research direction to develop anti-aging drugs.

The generation of T lymphocytes is adversely affected by ageing caused by thymic involution, which, together with changes in T-cell development, causes T-cell-dependent immunosenescence (Globerson and Effros 2000; Aspinall *et al*. 2002; Fry and Mackall 2002). The developmental potential of T-cell progenitors is not affected by aging; however, age-associated alterations in the thymic and extrathymic environment block their maturation (Montecino-Rodriguez *et al*. 2005; Zediak and Bhandoola 2005). Evidence shows that there are differences in the distribution of the main thymocyte populations, including DP thymocytes ($CD4^+CD8^+$), DN thymocytes ($CD4^-CD8^-$), SP $CD4^+$ thymocytes ($CD4^+CD8^-$), and SP $CD8^+$ thymocytes ($CD8^+CD4^-$). Thus, one result of ageing could be the selective loss of thymocyte populations. In the present study, the change tendency of thymocyte subsets in

Table 5: Percentage* of thymic Lymphocyte subsets for each group (%, mean ± SEM)

Group	Number	DN	$CD_4^+CD_8^+$	CD_4^+	CD_8^+	CD_4^+/CD_8^+
Young Control	8	3.36 ± 0.65^{a}	28.59 ± 1.04^{a}	58.08 ± 1.90^{a}	9.96 ± 0.65^{a}	5.83
RSA Control	8	$3.52 \pm 0.55^{a\,b}$	28.65 ± 0.90^{a}	58.35 ± 2.40^{a}	$9.48 \pm 1.16^{a\,b}$	6.15
AGE+ALT-711	8	$3.74 \pm 0.75^{a\,b}$	27.85 ± 0.87^{a}	59.47 ± 2.22^{a}	$8.93 \pm 0.89^{a\,b}$	6.70
AGEs Group	8	4.37 ± 0.64^{b}	21.85 ± 2.24^{c}	65.32 ± 2.55^{c}	$8.46 \pm 0.46^{b\,c}$	7.72
Aging Control	8	5.46 ± 0.82^{d}	19.60 ± 2.90^{d}	67.30 ± 2.13^{d}	7.63 ± 0.96^{c}	8.81

Note: The values with different letter differ significantly (with consecutive letter, $P < 0.05$) or very significantly (with interval letter, $P < 0.01$) and differ quietly (with same letter or unlabelled, $P > 0.05$. AGE, advance glycation end products; RSA, rat serum albumin; DN, double-negative; ALT-711, 4,5-dimethyl-3-(2-oxo-2-phenyl ethyl)-thiazol-3-ium chloride

*Percentages were calculated by the frequency of each group of positive cells separated from the total number of T lymphocytes, based upon the numbers presented in Fig. 3

Table 6: Relative *Rage* and *Notch1* mRNA expression (mean ± SEM.)

Group	Number	*Rage*	*Notch1*
Young Control	8	10.57 ± 2.78^{a}	9.69 ± 2.22^{a}
RSA control	8	10.42 ± 2.22^{a}	9.48 ± 1.18^{a}
AGE+ALT-711	8	12.07 ± 1.72^{a}	$8.56 \pm 1.20^{a\,b}$
AGE group	8	22.43 ± 6.63^{c}	$6.08 \pm 1.51^{c\,d}$
Aging Control	8	26.47 ± 3.57^{c}	4.77 ± 2.17^{d}

Note: The values with different letter differ significantly (with consecutive letter, $P < 0.05$) or very significantly (with interval letter, $P < 0.01$) and differ quietly (with same letter or unlabelled, $P > 0.05$. AGE, advance glycation end products; RSA, rat serum albumin; RAGE, receptor for advanced glycosylation end products; ALT-711, 4,5-dimethyl-3-(2-oxo-2-phenyl ethyl)-thiazol-3-ium chloride

aging rats compared with that young rats were consistent with the results of a previous study (Kozlowska *et al*. 2007), in which a significant increase in the percentage of DN and SP $CD4^+$ thymocytes, and a significant decrease SP and DP $CD8^+$ thymocytes were noted. We observed that the variation of T lymphocyte subsets in the young rats treated with AGEs was similar to that in aging rats and this trend could be reversed by treatment with ALT-711. The homeostatic stability of the immune system was destroyed in the rats treated with AGEs, which could provide important information leading to the prevention and cure of diabetes and other age-related diseases.

To explore the mechanism of the change in T lymphocyte subsets induced by AGEs, we detected the RAGE and Notch1 mRNA and protein expression levels. AGEs interact with specific cell surface-binding proteins to exert some of their effects. The best-characterized AGE receptor is RAGE, which is a multiligand member of the immunoglobulin superfamily (Yan *et al*. 1994). The Notch protein family comprises large transmembrane receptors with important functions in many developmental processes that act by controlling cell fate decisions. In cell-cell interactions, Notch receptors transduce signals that regulate the expression of proteins with important functions in differentiation and cell fate (Kimble and Simpson 1997). The human *NOTCH1* gene, encoding the mammalian homolog of Drosophila Notch, was first noted as participating in chromosomal translocations in combination with the T cell receptor β in a subset of human T cell leukemia (Ellisen *et al*. 1991). These translocations produced truncated Notch1 proteins lacking most of the extracellular domain, resulting in constitutively activated Notch signaling (Deftos *et al*. 2000). Notch-ligand engagement-mediated induction of two successive proteolytic cleavage events trigger this pathway. The second cleavage is performed by the γ-secretase activity of a Presenilin-containing complex, which releases the Notch intracellular domain (NICD). Activated Notch translocates into the nucleus, where it functions by binding to a transcriptional regulator (Bray 2006; Fiuza and Arias 2007).

The results of the previous study showed that Notch1 activation in $CD4^+CD8^+$ thymocytes enhanced the maturation of $CD4^+$ and $CD8^+$ thymocytes (Deftos *et al*. 2000). In NICD transgenic mice, activated Notch1 expression caused an increase in CD8 lineage T cells and a decrease in CD4 lineage T cells in developing T cells. These results led to the hypothesis that Notch functions in the CD4/CD8 T lineage decision (Robey *et al*. 1996; Fowlkes and Robey 2002). The observation that blocking Notch activity using γ-secretase inhibitors in fetal thymic organ culture had a marked impact on CD4/CD8 T lineage commitment, restraining CD8 SP development and promoting CD4 SP development, supported this hypothesis (Doerfler *et al*. 2001; Hadland *et al*. 2001).

This study provided evidence that rats treated with AGEs had high levels of RAGE mRNA and protein compared with those in the control group. This indicated that changes in T lymphocyte subsets, comprising increased CD4 SP thymocytes and decreased CD8 SP thymocytes, which are induced by AGEs, might participate in the RAGE signaling pathway. Furthermore, in the AGE and aging rats, the Notch1 mRNA and protein levels were reduced markedly compared with those in the control group. Thus, Notch1 signaling might promote variation in CD4+ and CD8+ T cell lineage development. The mechanism by which RAGE and Notch signaling combine to promote T cell subset differentiation requires further research. Notch frequently acts together with other signaling pathways, resulting in a wide variety of Notch-mediated cellular responses that are highly cell context-dependent. In

addition, we should determine how AGEs attenuate the expression of Notch1.

Conclusion

AGEs accelerated the aging process of the thymus and affected the development of thymic T lymphocyte subsets. These variations are consistent with the process of aging. The findings suggest that the effect of AGEs on certain diseases should be interpreted cautiously and serve as a reminder to clinicians to consider the clinical status of the elderly, especially those with diabetes. More research is required to confirm the mechanisms underlying the changes in thymic T lymphocyte subsets induced by AGEs, with the aim of promoting the immune status of aging populations, thus preventing or ameliorating age-related diseases.

Acknowledgements

We thank Dr. Guang Chen, Mrs. Lei Liu, Mr. Shi Wei Che, and Mr. Jia Nan Tao for their assistance with laboratory techniques. Thanks to the support of the project of North Medicine and functional Food Characteristics Subject in Heilongjiang Province.

References

Arslan B, E Culpan (2017). Effects of different gibberellic acid doses on seed yield, oil content and some quality traits of safflower (*Carthamus tinctorius* L.). *J Glob Innov Agric Soc Sci* 5:5–9

Aspinall R, D Andrew, J Pido-Lopez (2002). Age-associated changes in thymopoiesis. *In: Springer Semiinar In Immunopathology*, Vol. 24, pp: 87–101. Springer Berlin/Heidelberg, Germany

Bray SJ (2006). Notch signalling: a simple pathway becomes complex. *Nat Rev Mol Cell Biol* 7:678–689

Caruso C, S Buffa, G Candore, G Colonna-Romano, D Dunn-Walters, D Kipling, G Pawelec (2009). Mechanisms of immunosenescence. *Immun Ageing* 6:10

Cooper ME, V Thallas, J Forbes, E Scalbert, S Sastra, I Darby, T Soulis (2000). The cross-link breaker, N-phenacylthiazolium bromide prevents vascular advanced glycation end-product accumulation. *Diabetologia* 43:660–664

Deftos ML, E Huang, EW Ojala, KA Forbush, MJ Bevan (2000). Notch1 Signaling Promotes the Maturation of CD4 and CD8 SP Thymocytes. *Immunity* 13:73–84

Deng HB, CL Cheng, DP Cui, DD Li, L Cui, NS Cai (2006). Structural and Functional Changes of Immune System in Aging Mouse Induced by *D*-Galactose. *Biomed Environ Sci* 19:432–438

Doerfler P, MS Shearman, RM Perlmutter (2001). Presenilin-dependent γ-secretase activity modulates thymocyte development. *Proc Natl Acad Sci USA* 98:9312–9317

Ellisen LW, J Bird, DC West, AL Soreng, TC Reynolds, SD Smith, J Sklar (1991). TAN-1, the human homolog of the *Drosophila notch* gene, is broken by chromosomal translocations in T lymphoblastic neoplasms. *Cell* 66:649–661

Fiuza UM, AM Arias (2007). Cell and molecular biology of Notch. *J Endocrinol* 194:459–474

Fowlkes BJ, EA Robey (2002). A reassessment of the effect of activated Notch1 on CD4 and CD8 T cell development. *J Immunol* 169:1817–1821

Fry TJ, CL Mackall (2002). Current concepts of thymic aging. *In: Springer Seminar in Immunopathology*, Vol. 24, pp: 7–22. Springer Berlin/Heidelberg, Germany

Globerson A, RB Effros (2000). Ageing of lymphocytes and lymphocytes in the aged. *Immunol Today* 21:515–521

Gruver AL, LL Hudson, GD Sempowski (2007). Immunosenescence of ageing. *J.Pathol J Pathol Soc Great Brit Ireland* 211:144–156

Hadland BK, NR Manley, D Su, GD Longmore, CL Moore, MS Wolfe, EH Schroeter, R Kopan (2001). γ-Secretase inhibitors repress thymocyte development. *Proc Natl Acad Sci USA* 98:7487–7491

Hassan J, Q Maqsood, S Afzal, RD Khan, M Jamshaid (2017). Allelopathic potential of *Moringa oleifera* leaf extract to enhance the growth of sunflower (*Helianthus annuus* L.). *J Glob Innov Agric Soc Sci* 5:105–110

Kimble J, P Simpson (1997). The LIN-12/Notch signaling pathway and its regulation. *Annu Rev Cell Dev Biol* 13:333–361

Kozlowska E, M Biernacka, M Ciechomska, N Drela (2007). Age-related changes in the occurrence and characteristics of thymic CD4+ CD 25+ T cells in mice. *Immunology* 122:445–453

Lakatta EG, D Levy (2003). Arterial and cardiac aging: major shareholders in cardiovascular disease enterprises. Part I: aging arteries: a "set up" for vascular disease. *Circulation* 107:139–146

Leclerc E, G Fritz, M Weibel, CW Heizmann, A Galichet (2007). S100B and S100A6 differentially modulate cell survival by interacting with distinct RAGE (receptor for advanced glycation end products) immunoglobulin domains. *J Biol Chem* 282:17–31

Li JH, XR Huang, HJ Zhu, M Oldfield, M Cooper, LD Truong, RJ Johnson, HY Lan (2004). Advanced glycation end products activate Smad signaling *via* TGF-beta-dependent and independent mechanisms: implications for diabetic renal and vascular disease. *FASEB J* 18:176–178

Lynch HE, GL Goldberg, A Chidgey, MRMVD Brink, R Boyd, GD Sempowski (2009). Thymic involution and immune reconstitution. *Trends Immunol* 30:366–373

Montecino-Rodriguez E, H Min, K Dorshkind (2005). Reevaluating current models of thymic involution. *Sem Immunol* 17:356–361

Monnier M, V Vishwanath, KE Frank, CA Elmets, P Dauchot, RR Kohn (1986). Relation between complications of type I diabetes mellitus and collagen-linked fluorescence. *N Engl J Med* 314:403–408

Mueller J, GBD Re, H Buerki, HU Keller, MW Hess, H Cottier (1975). Nonspecific acid esterase activity: a criterion for differentiation of T and B lymphocytes in mouse lymph nodes. *Eur J Immunol* 5:270

Neeper M, AM Schmidt, J Brett, SD Yan, YC Pan, K Elliston, D Sernand, A Shaw (1992). Cloning and expression of a cell surface receptor for advanced glycosylation end products of proteins. *J Biol Chem* 267:14998–15004

Robey E, D Chang, A Itano, D Cado, H Alexander, D Lans, G Weinmaster, P Salmon (1996). An activated form of Notch influences the choice between CD4 and CD8 T cell lineages. *Cell* 87:483–492

Soulis-Liparota T, M Cooper, D Papazoglou, B Clarke, G Jerums (1991). Retardation by aminoguanidine of development of albuminuria, mesangial expansion, and tissue fluorescence in streptozocininduced diabetic rat. *Diabetes* 40:1328–1334

Stern D, SD Yan, SF Yanand, AM Schmidt (2002). Receptor for advanced glycation endproducts: a multiligand receptor magnifying cell stress in diverse pathologic settings. *Adv Drug Deliv Rev* 54:1615–1625

Surh CD, J Sprent (2008). Homeostasis of naive and memory T cells. *Immunity* 29:848–862

Tezel G, C Luo, X Yang (2007). Accelerated Aging in Glaucoma: Immunohistochemical Assessment of Advanced Glycation End Products in the Human Retina and Optic Nerve Head. *Invest Ophthalmol Vis Sci* 48:1201–1211

Tian J, K Ishibashi, K Ishibashi, K Reiser, R Grebe, S Biswal, P Gehlbach, JT Handa (2005). Advanced glycation endproduct-induced aging of the retinal pigment epithelium and choroid: A comprehensive transcriptional response. *Proc Natl Acad Sci USA* 102:11846–11851

Vasan S, X Zhang, X Zhang, A Kapurniotu, J Bernhagen, S Teichberg, J Basgen, D Wagle, D Shih, I Terlecky, R Bucala, A Cerami, J Egan, P Ulrich (1996). An agent cleaving glucose-derived protein crosslinks *in vitro* and *in vivo*. *Nature* 382:275–278

Vasileva V, Y Naydenova (2017). Nutritive value of forage biomass from mixtures of alfalfa with cocksfoot and tall fescue. *J Glob Innov Agric Soc Sci* 5:121–129

Wolffenbuttel BHR, CM Boulanger, FRL Crujns, MSP Huijberts, P Poitevin, GNM Swennen, S Vasan, JJ Egan, P Ulrich, A Cerami, BL Levy (1998). Breakers of advanced glycation end products restore large artery properties in experimental diabetes. *Proc Natl Acad Sci USA* 95:4630–4634

Yan SD, AM Schmidt, GM Anderson, J Zhang, J Brett, YS Zou, D Pinsky, D Stern (1994). Enhanced cellular oxidant stress by the interaction of advanced glycation end products with their receptors/binding proteins. *J Biol Chem* 269:9889–9897

Zediak VP, A Bhandoola (2005). Aging and T cell development: interplay between progenitors and their environment. *Sem Immunol* 17:337–346

Zulfiqar U, M Ishfaq, MU Yasin, N Ali, M Ahmad, A Ullah, W Hameed (2017). Performance of maize yield and quality under different irrigation regimes and nitrogen levels. *J Glob Innov Agric Soc Sci* 5:159–164